Hydrothermal Reactivity of Na-*n*-Micas ($n = 2, 3, 4$)

María D. Alba, Miguel A. Castro,* Moisés Naranjo, and Esperanza Pavón

Departamento de Química Inorgánica, Instituto de Ciencia de Materiales, Universidad de Sevilla, Consejo Superior de Investigaciones Científicas, Avenida Américo Vespucio s/n. 41092 Sevilla, Spain

Received July 8, 2005. Revised Manuscript Received February 24, 2006

High charge mica samples, with layer charge values between 2 and 4, have been synthesized via the sodium chloride melt procedure, and their hydrothermal reactivities for the formation of lutetium disilicate have been evaluated. Characterization of the synthesized micas, through a combination of techniques that inform of both the long and the short range order of the solids, indicates a progressive incorporation of aluminum in the tetrahedral sheet as the layer charge increases. Hydrothermal treatment of the synthesized samples causes the reaction between the lanthanide ions in the solution and the tetrahedral silicate species from the micas to form a new crystalline lanthanide disilicate phase. Those samples with higher layer charge show the higher reactivity, in accordance with our initial hypothesis. In conclusion, these samples have a novel and attractive application through a new reaction mechanism, of special relevance for the storage of high activity radioactive waste.

Introduction

The study of the interaction between exchangeable ions and layered silicates under thermal and hydrothermal treatments is central to the evaluation of the physicochemical properties of these materials. Mechanisms describing the interaction of multivalent cations with clay minerals, after mild thermal and hydrothermal treatments, have been classically based on their rheological properties and ion-exchange capacities.[1] However, a new kind of interaction mechanism in which, operating under mild hydrothermal conditions, the interlayer cations and the silicon atoms of the clay react to produce new disilicate crystalline phases has recently been described.[2] This new interaction is of particular importance to several applied fields, such as catalysis, adsorption, waste immobilization, and detergency. In particular, the role of the 2:1 layered silicates in the highly radioactive nuclear waste immobilization, through this new mechanism, has been examined.[3−5] Two structural features were identified as mainly responsible for the enhanced reactivity: the amount of tetrahedral substitutions and the trioctahedral nature of the octahedral sheet of the layers.

To explore this hydrothermal reactivity, a family of layered silicates complying with the structural requisites mentioned above has been pursued. Na-4-mica is a highly charged expandable sodium fluorophlogopite first reported by Gregorkiewitz and Rausell-Colum, which has been described as a trioctahedral mica-type 2:1 layered silicate with half of the tetrahedral sites occupied by aluminum ions.[6] Recently, other members with different layer charge values, ranging from 2 to 4 units per cell, have been synthesized.[7] These swelling high-charge micas, in which the layer charge value can be adjusted, could be valuable not only for the decontamination of harmful divalent and heavy metal cations via ion-exchange reaction[8] but also for the selective removal of highly radioactive ions.

From the report published by Gregorkiewitz,[8] in which just small quantities (∼20 mg) of sample were obtained from fluoride melts, several studies have been carried out to develop easier and more productive synthesis routes, determining the exchange behavior of the synthesized micas and recycling fly ashes through the synthesis of high-charge micas.[9] Regarding the procedure of preparation, some progress has been attained. Large amounts of Na-4-mica flakes with a small and uniform particle size were obtained through the method proposed by Paulus et al.,[10] and a simplification of this method by using fumed silica as the silicon source was reported by Franklin and Lee.[11] Later, synthesis of Na-4-mica from calcined kaolinite, a cheap aluminosilicate source, was described, and the method was employed to prepare high charge micas with layer charge values between 2 and 4 unit charges per unit cell.[12−14] Unfortunately, these synthesis methods employ excess amounts of NaF, which still require further washing with boric acid saturated solutions to remove any insoluble fluorides and subsequent substitution of exchangeable Na^+

(1) Figueras, F. *Catal. Rev. Sci. Eng.* **1988**, *30*, 457.
(2) Trillo, J. M.; Alba, M. D.; Alvero, R.; Castro, M. A.; Muñoz-Paez, A.; Poyato, J. *Inorg. Chem.* **1994**, *33*, 3861.
(3) Alba, M. D.; Becerro, A. I.; Castro, M. A.; Perdigón, A. C. *Am. Miner.* **2001**, *86*, 115.
(4) Alba, M. D.; Becerro, A. I.; Castro, M. A.; Perdigón, A. C. *Am. Miner.* **2001**, *86*, 124.
(5) Becerro, A. I.; Naranjo, M.; Alba, M. D.; Trillo, J. M. *J. Mater. Chem.* **2003**, *13*, 1835.
(6) Gregorkiewitz, M.; Rausell-Colom, J. A. *Am. Miner.* **1987**, *72*, 515.
(7) Komarneni, S.; Kozai, N.; Paulus, W. J. *Nature* **2001**, *410*, 771.
(8) Kodama, T.; Komarneni, S. *J. Mater. Chem.* **1999**, *9*, 533.
(9) Park, M.; Lee, D. H.; Choi, C. L.; Lim, W. T.; Lee, S. K.; Heo, N. H.; Komarneni, S.; Choi, J. *J. Porous Mater.* **2002**, *9*, 291.
(10) Paulus, W. J.; Komarneni, S.; Roy, R. *Nature* **1992**, *357*, 571.
(11) Franklin, E. R.; Lee, E. *J. Mater. Chem.* **1996**, *6*, 109.
(12) Komarneni, S.; Pidugu, R.; Amonette, J. E. *J. Mater. Chem.* **1998**, *8*, 205.
(13) Kodama, T.; Higuchi, T.; Shimizu, T. Shimizu, K.; Komarneni, S.; Hoffbauer, W.; Schneider, H. *J. Mater. Chem.* **2001**, *11*, 2072.
(14) Kodama, T.; Hasegawa, K.; Shimizu, K.; Komarneni, S. *Sep. Sci. Technol.* **2003**, *38*, 679.

10.1021/cm0514802 CCC: $33.50
Published on Web 05/16/2006

by H^+ ions from boric acid. Very recently, a new method for the synthesis of Na-4-mica, in which NaCl and MgF_2 were employed to avoid the excess of NaF, has been described.[15] However, this method has only been employed in the preparation of Na-4-mica, micas with other layer charge values not being yet prepared. Additionally, further characterization of fundamental aspects of the prepared sample such as the local environment of the tetrahedral atoms is necessary.

The objectives of the present paper are (a) to synthesize Na-*n*-micas, $n = 2$, 3, and 4, from a unique procedure; (b) to characterize the obtained solids by means of powder X-ray diffraction (XRD) and multinuclear magic angle spinning nuclear magnetic resonance (MAS NMR), special attention being paid to the local order of the tetrahedral aluminum ions, allowing us to examine the proposed mechanism; and (c) to evaluate the hydrothermal reactivity of the solids and their efficiency for the immobilization of highly radioactive ions through the use of a reaction extensively studied by us, the hydrothermal formation of lutetium disilicate.

Experimental Section

Synthesis Method. A procedure similar to that described by Park et al. was employed in all the cases.[17] Near-stoichiometric powder mixtures with the molar compositions $(8 - n)SiO_2$, $(n/2)Al_2O_3$, $6MgF_2$, and $(2n)NaCl$ were used for the synthesis of Na-*n*-micas ($n = 2$, 3, 4). Starting materials employed were SiO_2 from Sigma (CAS no. 112945-52-5, 99.8% purity), $Al(OH)_3$ from Riedel-de Haën (CAS no. 21645-51-2, 99% purity), MgF_2 from Aldrich (CAS no. 20831-0, 98% purity), and NaCl from Panreac (CAS no. 131659, 99.5% purity). All the reactant mixtures were vigorously ground and subsequently heated in Pt crucibles at 900 °C for 15 h. After cooling, the solids were washed with deionized water and dried at room temperature.

Hydrothermal treatments were carried out by mixing 300 mg of each sample with 30 mL of 4.35×10^{-2} M $Lu(NO_3)_3$ solutions, lutetium being employed as a actinide simulator, in accordance with previous reports.[16] The suspensions were hydrothermally treated in quartz vessels closed in stainless steel reactors at 300 °C for 48 h. After cooling at room temperature, the reactors were opened and the treated solids were washed with deionized water and dried at room temperature.

Characterization. The obtained solids before and after the hydrothermal treatments were characterized by means of XRD, ^{29}Si, ^{27}Al, ^{1}H, and ^{23}Na MAS NMR, and thermogravimetric and differential thermal analysis (TG/DTA).

XRD patterns were obtained with a Siemens Kristaloflex D500 instrument, Cu Kα radiation, at 40 kV and 40 mA, and diffracted beam monochromated with graphite. Diffractograms were obtained from 3 to 70° 2θ at a scanning speed of 1° 2θ/min with a scan step of 0.05° 2θ. General procedures, such as the Le Bail fit as included in the GSAS software package,[17] were employed to index the XRD peaks and to refine the cell parameters of the synthesized micas.

Single-pulse (SP) MAS NMR experiments were recorded on a Bruker DRX400 spectrometer equipped with a multinuclear probe.

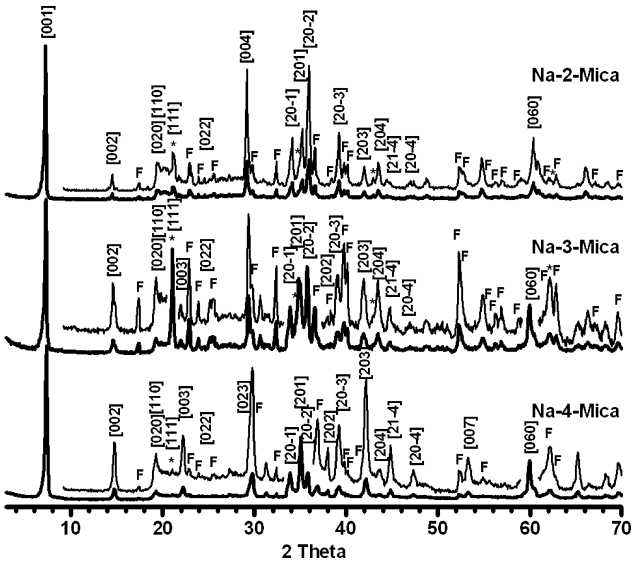

Figure 1. XRD patterns for the Na-*n*-mica samples, $n = 2$, 3, 4. F: Forsterite. *: Sodium aluminosilicate.

Powdered samples were packed in 4 mm zirconia rotors and spun at 12 kHz.

^{1}H MAS spectra were obtained using typical $\pi/2$ pulse widths of 4.1 μs and a pulse space of 5 s. ^{29}Si MAS NMR spectra were acquired at a frequency of 79.49 MHz, using a pulse width of 2.7 μs ($\pi/2$ pulse length = 7.1 μs) and a delay time of 3−60 s. ^{27}Al MAS NMR spectra were recorded at 104.26 MHz with a pulse width of 0.92 μs ($\pi/2$ pulse length = 9.25 μs) and a delay time of 0.1 s. ^{23}Na MAS NMR spectra were recorded at 105.84 MHz with pulse widths of 2.0 μs ($\pi/2$ pulse length = 12.0 μs) and delay times of 0.1 s. The chemical shift values were reported in ppm from tetramethylsilane for ^{29}Si and ^{1}H, from a 0.1 M solution of $AlCl_3$ for ^{27}Al, and from 0.5 M solutions of NaCl for ^{23}Na.

TG/DTA experiments were carried out using a Seiko TG-DTA EXSTAR 6300 instrument, with alumina as the reference. The samples were placed into platinum crucibles and maintained at air throughout the heating period, and the temperature was increased at a constant rate of 8 °C/min.

Results and Discussion

Characterization of the Synthesized Na-*n*-Micas. Figure 1 shows the XRD patterns obtained for the Na-4-mica, Na-3-mica, and Na-2-mica, respectively. The displayed patterns are qualitatively similar and can be described in terms of two kinds of reflections: first, a group of them, which includes most of the reflections observed, can be attributed to the hydrated mica phase, and second, a less numerous group of reflections is attributed to impurities.

In the three products, the predominant form was the one-layer hydrate mica with a [001] reflection centered at 7.25−7.35° 2θ, corresponding to a spacing value of 12.19−12.03 Å, and with strong 00*l* reflections compatible with layered structures. Likewise, the unit cell dimensions obtained for the three phases (Table 1) indicate a structure based on a mica-type structure, and they are very similar to those reported previously.[8] It is notable the negligible presence of the anhydrous phase and the constant *c*-axis value obtained in all the cases. The three patterns differ in the relative peak intensities, probably due to differences in composition, crystal shape and size, and crystallinity of the products.

(15) Park, M.; Lee, D. H.; Choi, C. L.; Kim, S. S.; Kim, K. S.; Choi, J.*Chem. Mater.* **2002**, *14*, 2582.
(16) Muñoz-Paez, A.; Alba, M. D.; Castro, M. A.; Alvero, R.; Trillo, J. M. *J. Phys. Chem.* **1994**, *98*, 9850.
(17) Larson, A. C.; Von Dreele, R. B. *GSAS: General Structural Analysis system*; Los Alamos National Laboratory: Los Alamos, NM, 1994 (The Regents of the University of California).

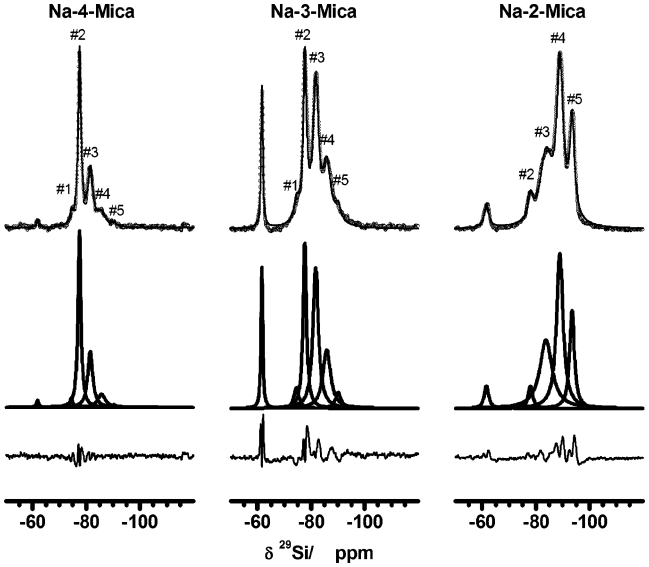

Figure 2. ^{29}Si MAS NMR spectra for the Na-*n*-mica samples, *n*= 2, 3, 4. Each graph includes the experimental spectrum (upper), the set of simulated contributions as described in the text (medium), and the residuals (lower).

Table 1. Calculated Cell Parameters for Hydrated Na-*n*-Micas (*n* = 4, 3, and 2)

cell parameter	Na-4-mica	Na-3-mica	Na-2-mica
a (Å)	5.3488(4)	5.3497(3)	5.3517(3)
b (Å)	9.2536(11)	9.2522(4)	9.2545(6)
c (Å)	12.0565(11)	12.0564(6)	12.0444(8)
β (deg)	94.214(11)	94.215(4)	94.200(6)
cell volume (Å^3)	595.13(17)	595.17(9)	594.92(11)

Regarding the impurities, in accordance with previous reports,[17] two different phases can be identified, and their reflections are indicated in Figure 1 as F for the forsterite phase (Mg_2SiO_4, JCPDS no. 34-0189) and as asterisks for the sodium aluminosilicate phase ($Na_6Al_4Si_4O_{17}$, JCPDS no. 49-0004). Although both phases are present in the three solids, the reflection intensities are different in each sample, the Na-4-mica diagram exhibiting the weakest peaks for the impurities.

Thermal analysis for the three products has been carried out both to analyze the dehydration processes occurring during the heating of the materials and to investigate the presence of other components in the solids, the results showing only an interlayer dehydration process, compatible with the proposed structure.

^{29}Si MAS NMR measurements have been performed for the three synthesized specimens and are shown in Figure 2 along with their fitting profiles and residues. This figure includes the ^{29}Si MAS NMR spectra for a set of Na-*n*-micas synthesized under the same experimental procedure. All the spectra can be described in terms of three different kinds of signals. First, a broad band within the range between −70 and −90 ppm is compatible with the existence of several single Q^3(*n*Al) environments as expected for 2:1 layered aluminosilicates.[18] Table 2 includes the fitting parameters used for each contribution, and a change in both the position and the relative intensity as the Si/Al ratio varies is observable. Both changes can be attributed to the variation in the layer charge obtained for each solid, in accordance with well-established results,[18] but the number of signals, five in the case of Na-4-mica and Na-3-mica, deserves further explanation. Second, a signal centered at about −61.7 ppm appears in the three spectra previously assigned to Q^0 silicon environments from forsterite impurity,[19] which was also detected from XRD diagrams. Because the relaxation time for forsterite is higher than the delay time used in acquiring these spectra, it is not possible to determine precisely the forsterite fraction in each sample. However, intensity ratios observed in the spectra are in accordance with the previous XRD data, Na-4-mica being the purest one. And third, the sodium aluminosilicate phase should produce a Si signal at around −84 ppm,[20] which is overlapped with the Q^3(*n*Al) environments from micas. This overlapping should account for the broadening in the fitting line centered at this position in each spectrum.

Table 2. Signal Parameters from ^{29}Si NMR Spectra for Hydrated Na-*n*-Micas (*n* = 4, 3, and 2)

	Na-4-mica			Na-3-mica			Na-2-mica		
peak	−*δ* (ppm)	fwhm (ppm)	*A* (au)	−*δ* (ppm)	fwhm (ppm)	*A* (au)	−*δ* (ppm)	fwhm (ppm)	*A* (au)
1	74.46	1.14	0.10	74.56	2.20	0.40			
2	77.49	1.28	1.98	77.69	1.52	2.20	78.01	2.00	0.40
3	81.51	2.20	1.07	81.76	2.40	2.95	83.80	5.50	3.30
4	85.68	3.45	0.40	85.88	3.44	1.76	88.97	2.85	3.87
5	90.32	1.98	0.05	90.12	2.50	0.35	93.50	2.10	1.80

Previous ^{29}Si MAS NMR spectra have been reported from both natural and synthetic high charge micas. However, while a unique signal, compatible with Q^3(3Al) environments associated to a fully ordered tetrahedral structure, is observed for the natural high charge margarite mica,[20] more than one contribution is present in the spectra recorded from synthetic Na-4-mica and Na-2-mica samples.[14,17,21,22] It is interesting to note that whereas the four distinct Si signals in the Na-2-mica spectrum are assigned to Si(0Al), Si(1Al), Si(2Al), and Si(3Al) environments, the expected adherence to Lowenstein rule leads to assignment of the different Si signals observed from Na-4-mica samples as due to either several Si(3Al) environments[17] or a mixture of Si(3Al) and Si(2Al) environments.[24] In any case, the nature of these different Si environments in these synthetic micas is not well-understood.

A general comparison of the three experimental spectra indicates that (a) a variation in the different Si environments occurs, in agreement with the Si/Al ratio; (b) a fifth peak at about −74.5 ppm appears for the Na-3- and Na-4-micas. For the latter, if a 1:1 Si/Al ratio is assumed, just two possibilities are expected: (1) a homogeneous Si−Al distribution without Al−O−Al linkages, such as that observed for the natural margarite mica, and (2) any other distribution, maintaining the 1:1 Si/Al ratio should cause the appearance of Al−O−

(18) Sanz, J.; Serratosa, J. M. *J. Am. Chem. Soc*. **1984**, *106*, 4790.
(19) Mägi, M.; Lippmaa, M.; Samoson, A.; Englehardt, G.; Grimmer, A. R. *J. Phys. Chem.* **1984**, *88*, 1518.
(20) Engelhardt, G.; Michel, D. *High Resolution Solid State NMR of Silicates and Zeolites*; Wiley: New York, 1987.
(21) Komarneni, S.; Pidugu, R.; Hoffbauer, W.; Scheneider, H. *Clays Clay Mineral*. **1999**, *47*, 410.
(22) Stout, S. A.; Komarneni, S. *J. Mater. Chem.* **2003**, *13*, 377.
(23) Alba, M. D.; Becerro, A. I.; Castro, M. A.; Perdigón, A. C. *Chem. Commun.* **2000**, *1*, 37.
(24) Alba, M. D.; Becerro, A. I.; Castro, M. A.; Perdigón, A. C.; Trillo, J. M. *J. Phys. Chem. B* **2003**, *107*, 3996.

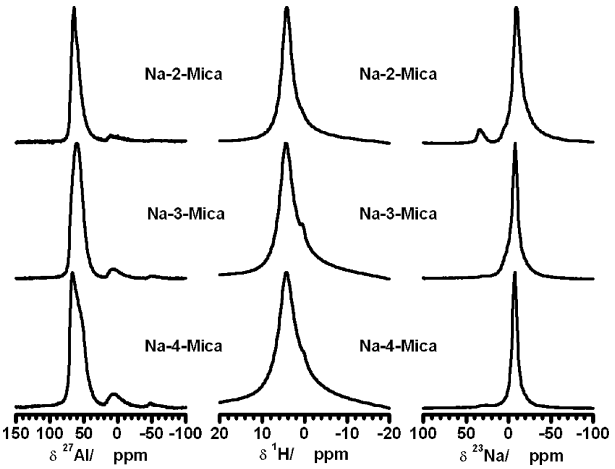

Figure 3. ^{27}Al (left), ^{1}H (center), and ^{23}Na (right) MAS NMR spectra for the Na-*n*-mica samples, $n = 2, 3, 4$.

Al linkages. While the first possibility leads to the existence of just one single Si environment and just one ^{29}Si MAS NMR signal, the second case leads to the existence of more Si environments and more than one ^{29}Si MAS NMR signal. In consequence, the acceptance of equal amounts of Si and Al in the tetrahedral layer along with the observation of several Si signals in the NMR spectra suggests that these samples, in the case that they have a Si:Al ratio close to 1, do not obey Lowenstein's rule.

To deepen our knowledge of the local order of these systems, other NMR-active nuclei have been incorporated in this study. Figure 3 includes ^{27}Al, ^{1}H, and ^{23}Na MAS NMR spectra from Na-4-mica, Na-3-mica, and Na-2-mica. These measurements are complementary and provide useful information about the different local environments of these species in the solids.

Regarding the ^{27}Al MAS NMR spectra (left column), all the samples show the presence of an asymmetric band at about 67 ppm corresponding to aluminum in tetrahedral coordination.[20] Likewise, a peak centered at about 0 ppm, arising from octahedral coordination,[20] is observed in the three samples, its contribution being higher as the Si/Al ratio decreases. Regarding tetrahedral environments, ^{27}Al NMR signals in Na-4-micas with two components have been previously identified, although they have not been interpreted.[14] The sodium aluminosilicate phase, identified from XRD and ^{29}Si MAS NMR measurements, could be responsible for this result. Alternatively, if Al−O−Al linkages were present, more than one Al environment would be expected, more evident for those samples having lower Si/Al ratios. In the case of octahedral environments, a small amount of Al incorporated in octahedral sheets has already been reported in Na-4-micas, Al replacing Mg.[14,23] As a result of the two different octahedral positions Al can occupy in micas and interlayer and structural octahedral sites, homoionization experiments with both Mg and Na ions were carried out to elucidate the actual positions of Al. Undistinguishable Al spectra were recorded from samples after homoionization treatments, with octahedral Al environments, Al ions being identified in octahedral sheets, in accordance with the literature.

^{1}H MAS NMR spectra have been recorded from the samples (central column) because they provide useful information on the location of the different proton sites and are related with the octahedral nature of the layers.[23,24] The ^{1}H NMR spectra shows two components as reported previously for 2:1 layered aluminosilicates and attributed to interlayer water and hydroxyl groups, respectively. While the water signal, centered at 4.1 ppm, can be unequivocally assigned to interlayer water in these samples and their chemical shifts values are in agreement with those observed for other Na-saturated layered aluminosilicates, the assignment of the second component, centered at 0.5 ppm as expected for hydroxyl groups in trioctahedral samples, is uncertain due to the theoretical fluorophlogopite composition. This component is more evident for Na-3-mica and Na-4-mica samples and could be caused by the incorporation of OH species during the hydration process performed after the synthesis.

Finally, ^{23}Na MAS NMR spectra from the samples have been included at Figure 3 (right column). A main peak centered at about −8 ppm is present in the three spectra and can be attributed to hydrated Na ions located in the interlayer space of micas, in accordance with similar results reported for Na-ZSM-5 zeolite.[25] Additionally, two different signals can be identified in the spectra: a shoulder at around 0 ppm is observed for Na-2-mica and Na-3-mica samples, probably caused by the Na aluminosilicate phase, and a signal at around 30 ppm, more evident from Na-2-mica, caused by the NaCl precursor employed in the synthesis and previously measured as a pure solid in our equipment. In summary, these spectra clearly show that almost all Na ions were incorporated in the interlayer sites as hydrated exchangeable cations, as expected for Na-saturated micas.

Hydrothermal Reactivity of the Na-*n*-Micas. To fulfill the third objective of the present paper, Na-*n*-mica samples were submitted to hydrothermal treatments in contact with Lu ions solutions at 300 °C for 48 h, in which the Lu ion concentration was selected from the Na-4-mica chemical formula to allow a theoretically complete consumption of Si atoms. Although our first hydrothermal assays were performed on lanthanide-saturated silicates,[26] we have recently modified the hydrothermal procedure by heating natural ion-exchanged silicates in contact with lanthanide ion solutions because this situation resembles more adequately the expected scenario in the projected geological barriers to immobilize radionuclide wastes.[27]

Figure 4 shows XRD patterns from Na-*n*-micas hydrothermally treated. All the diagrams can be described in terms of three kinds of crystalline phases. First, diffraction peaks corresponding to remaining structures, forsterite (JCPDS no. 34-0189) and mica, are observed and marked with asterisks in the figure. Second, the target structure, $Lu_2Si_2O_7$, accounts for peaks marked with ∧ symbols (JCPDS no. 35-0326), which exhibits different intensities depending on the sample. And third, the rest of the observed diffraction peaks are

(25) Ohgushi, T.; Kawanabe, Y. *Zeolites* **1994**, *14*, 356.
(26) Alba, M. D.; Alvero, R.; Becerro, A. I.; Castro, M. A.; Muñoz-Paez, A.; Trillo, J. M. *J. Phys. Chem.* **1996**, *100*, 19559.
(27) Perdigón, A. C. Thesis, University of Sevilla, Sevilla, Spain, 2002.

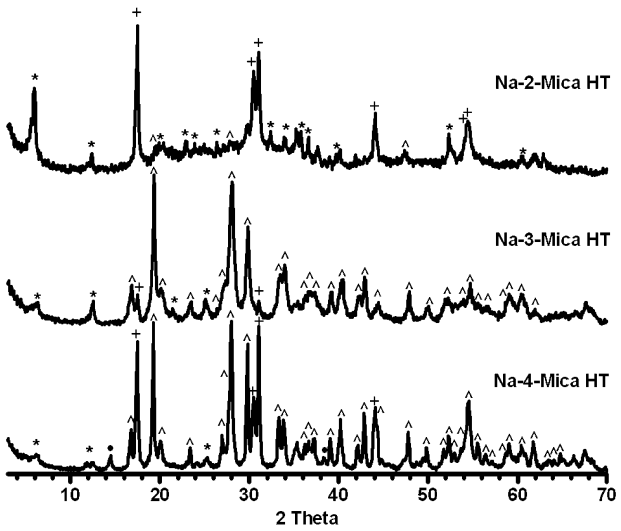

Figure 4. XRD patterns for the Na-*n*-mica samples, $n = 2, 3, 4$, hydrothermally treated in lutetium nitrate solutions at 300 °C for 48 h. ∧: Lutetium disilicate. +: $NaLuF_4$. ●: AlOOH. *: Forsterite and mica.

interpreted as due to the appearance of two new crystalline phases: $NaLuF_4$ (JCPDS no. 27-0726), observed in all the cases and marked with +, and AlOOH (JCPDS no. 05-0190), marked with ●, only observed in the treated Na-4-mica sample.

Regarding the initial layered silicate structure, a clear disruption is observed for all the samples, although a relationship between the extent of the degradation and the mica layer charge value is observed. While a set of mica diffraction peaks, including basal and structural reflections, is still present for the Na-2-mica, only two clear basal reflections centered at around 6° and 12° 2θ are shown for the Na-3-mica and Na-4-mica. These results indicate a larger structural disruption as the layer charge increases.

Simultaneously to this effect, a progress in the appearance of the new lutetium disilicate phase occurs. The diffraction diagrams range from the incipient presence of reflections corresponding to the $Lu_2Si_2O_7$ phase for the Na-2-mica to an extensive formation of this phase for the Na-4-mica, in which all the reported reflections are observed. These results are consistent with our initial hypothesis about the link between the degree of tetrahedral substitution in the layer and the hydrothermal reactivity of the samples. Because ^{29}Si MAS NMR results for the initial samples do not indicate a fully ordered tetrahedral structure, a reduction in the hydrothermal reactivity as the Si:Al ratio moves closer to 1:1 is not expected. In consequence, the Na-4-mica sample is an optimum candidate for this reaction.

Finally, the hydrothermal reaction causes in all the samples the generation of the $NaLuF_4$ phase, not observed in our similar hydrothermal treatments in smectites.[5] This fact might be associated with the fluorinated character of these samples.

Figure 5 exhibits ^{29}Si MAS NMR spectra for the Na-*n*-mica samples hydrothermally treated. A new contribution, centered at −91.6 ppm in the three cases,[6] compatible with the new $Lu_2Si_2O_7$ phase reported from the XRD results, is shown. No evidence of other new contributions is observed, the unique reaction deduced for silicon atoms being the formation of the disilicate phase. It is remarkable that even

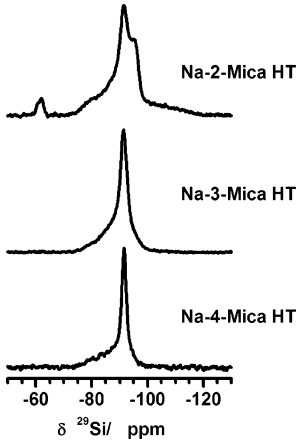

Figure 5. ^{29}Si MAS NMR spectra for the Na-*n*-mica samples, $n = 2, 3, 4$, hydrothermally treated in lutetium nitrate solutions at 300 °C for 48 h.

in the Na-2-mica sample the main contribution to the ^{29}Si MAS NMR spectrum is the disilicate signal, in contrast with the only appearance of a few incipient XRD peaks for this phase. The $Lu_2Si_2O_7$ formation is a general reaction in all the samples, although its extent, as deduced from the XRD long-range order study, is dependent on the amount of tetrahedral substitution in each sample. Along with the disilicate signal, the ^{29}Si MAS NMR spectra contain a remaining profile from the layered silicate structure in the three samples. Again, this profile is more clearly observable in the Na-2-mica, in accordance with the XRD pattern, in which a larger fraction of the mica structure is preserved after the hydrothermal treatment, and it is almost absent in the Na-4-mica sample, in which a nearly complete consumption of the mica structure happens. This sample is, therefore, an optimum candidate for this chemical process and validates our initial hypothesis.

Finally, the MAS NMR signals arising from the minor elements aluminum and sodium, not shown in the figure, are compatible with the rest of the results. On one hand, ^{27}Al signals show two different Al environments, attributed to tetrahedral and octahedral coordination, which show a Al(VI)/Al(IV) intensity ratio increasing as the initial layer charge of the sample increases. This fact is in agreement with the expected course of the reaction: those more reactive samples, in which a higher structural disruption happens, should cause a higher transformation in the aluminum environment and, consequently, a higher reduction of the initial tetrahedral environment. In the case of the Na-4-mica, not only the highest Al(VI)/Al(IV) intensity ratio is observed, but its spectrum is accompanied by a diffraction pattern compatible with a new AlOOH crystalline phase. On the other hand, ^{23}Na MAS NMR spectra recorded using the same scan number as in the initial sample show a very low S/N ratio, clearly indicating the almost disappearance of Na atoms in the products. They should be dissolved in the washing process performed after the treatment, and they should be only partially incorporated in the $NaLuF_4$ phase detected from XRD results.

Concluding Remarks

The NaCl melt method can be considered as a general procedure for the synthesis of high layer charge layer

silicates. The described method allows the layer charge of the sample MAS NMR spectra from the mica samples to be tuned, indicating the avoidance of Lowenstein rules for the sample with a Si:Al ratio close to 1.

The hydrothermal treatments of all the samples lead to the formation of $Lu_2Si_2O_7$, the reaction being extensive in the case of the Na-4-mica sample. This fact validates our initial hypothesis on the structural features responsible for the hydrothermal reactivity of layered silicates. Therefore, Na-4-mica can be considered an appropriate material for the decontamination of heavy metal cations not only through an ion exchange reaction but also through the formation of new crystalline disilicate phases.

Acknowledgment. We gratefully acknowledge the DGCYT (MAT2002-03504 and CTQ2004-05113 Projects) for financial support and X-Ray Laboratory at CITIUS, Universidad de Sevilla, and Solid State NMR Service at CICIC, CSIC, for the use of their experimental facilities. We also acknowledge Prof. Mike Simon for his useful comments on the English style of the manuscript.

CM0514802